ACS Medicinal Chemistry Letters

Letter

Design and Synthesis of Novel meta-Linked Phenylglycine Macrocyclic FVIIa Inhibitors.

Jeremy M. Richter, Daniel L. Cheney, J. Alex Bates, Anzhi Wei, Joseph M Luettgen, Alan R. Rendina, Timothy M. Harper, Rangaraj Narayanan, Pancras C Wong, Dietmar A Seiffert, Ruth R. Wexler, and Eldon Scott Priestley

ACS Med. Chem. Lett., **Just Accepted Manuscript** • DOI: 10.1021/acsmedchemlett.6b00375 • Publication Date (Web): 01 Nov 2016

ACS Publications

ACS Medicinal Chemistry Letters is published by the American Chemical Society. 1155 Sixteenth Street N.W., Washington, DC 20036

Design and Synthesis of Novel *meta*-Linked Phenylglycine Macrocyclic FVIIa Inhibitors.

Jeremy M. Richter*, Daniel L. Cheney, J. Alex Bates, Anzhi Wei, Joseph M. Luettgen, Alan R. Rendina, Timothy M. Harper, Rangaraj Narayanan, Pancras C. Wong, Dietmar Seiffert, Ruth R. Wexler, E. Scott Priestley.

Bristol-Myers Squibb Research & Development, Hopewell, New Jersey, 08534, United States

KEYWORDS FVIIa, Factor VIIa, macrocycle, thrombosis, antithrombotic, anticoagulant.

ABSTRACT: Two novel series of *meta*-linked phenylglycine-based macrocyclic FVIIa inhibitors have been designed to improve the rodent metabolic stability and PK observed with the precursor *para*-linked phenylglycine macrocycles. Through iterative structure-based design and optimization, the TF/FVIIa K_i was improved to sub-nanomolar levels with good clotting activity, metabolic stability, and permeability.

Cardiovascular diseases remain the leading cause of death worldwide in both developed and developing nations. Many of these deaths can be attributed to arterial or venous thrombosis (*e.g.* myocardial infarction, ischemic stroke, pulmonary embolism, and deep vein thrombosis).[1] In light of this high level of medical need, the discovery of novel and selective antithrombotic therapies with high efficacy and low bleeding liability would be beneficial.

Factor VIIa (FVIIa) resides at the beginning of the extrinsic coagulation cascade.[2] When blood vessel walls are compromised, tissue factor (TF) is exposed to circulating FVIIa, leading to the conversion of FIX to FIXa. Both FIXa and FVIIa (in conjunction with their cofactors FVIIIa and tissue factor, respectively) cause the conversion of FX to FXa, which in turn converts prothrombin to thrombin. Thrombin then promotes clot formation by converting fibrinogen to fibrin and activating platelets, generating an extended fibrin/platelet network.[3]

Various blood coagulation factors have been the target of pharmaceutical small molecule inhibitor research; including, most notably FXa (e.g. apixaban and rivaroxaban) and thrombin (e.g. dabigatran).[4] FVIIa inhibitors are appealing as anticoagulant therapies for several reasons. First, the efficacy and safety of FVIIa disruption has been demonstrated clinically with recombinant nematode anticoagulant protein c2.[5-7] Secondly, it has been demonstrated preclinically that FVIIa inhibition has excellent efficacy and limited bleeding liability.[8-15] This profile has made FVIIa a tantalizing target for anticoagulant therapy for many years[16-20] and has provided the impetus for the investigations detailed herein.

Of particular interest while considering the design of novel FVIIa inhibitors are the two polar residues (Asp189 and Ser190) that reside at the bottom of the primary specificity pocket (S1). Historically, benzamidines are typically required to bind to these residues and confer the required level of potency; however, this comes at a cost of poor permeability and oral bioavailability, necessitating a prodrug strategy.[20-23] We have previously reported structures such as **1** that contain weakly-basic benzamidine replacements that confer improvements in permeability and oral exposure while maintaining good of potency.[24-26] This series of compounds exhibited many favorable properties; however, low rodent oral bioavailability was a key limitation. Biotransformation studies traced this poor exposure to the carbamate upper linker in these macrocycles, which was highly metabolized in rodent liver microsomes. Therefore, in an effort to design inhibitors that retained favorable potency and selectivity, and incorporated improved metabolic stability and oral bioavailability, a program was initiated to modify the macrocyclic upper linker.[27]

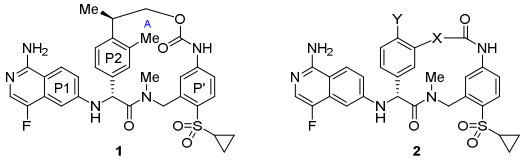

FVIIa K_i (37 °C): 0.43 nM
FVIIa defPT: 6.1 μM
PAMPA (pH 7.4, 5.5): 1100, 900 nm/s
H,D,RLM $t_{1/2}$: 45, 26, 1.9 min
Dog PK: F = 40%, Cl = 8 mL/min/kg
Rat PK: F = <5%

Figure 1. General structures of FVIIa inhibitors.

The previously reported *para*-linked macrocycles (e.g. **1**) make several critical contacts with the FVIIa active site,[24-26] leading to the exquisite potency observed. When designing novel macrocyclic inhibitors, we were cognizant of the fact that these interactions would need to be maintained or even improved in order to retain the desired potency. One such interaction that would need to be considered was the hydrophobic contact with the S2 binding pocket, which is primarily made by the P2-methyl group labeled as "A" in structure **1**. It was reasoned that macrocycles linked at the *meta* position, instead of the *para* position, of the P2-aryl ring could maintain this favorable hydrophobic contact while significantly altering the linker constitution and modulating the metabolic profile.

This publication details the design and synthesis of structures of type **2**, which provided a novel scaffold for further elaboration.

Initial efforts surrounding the new chemotype **2** required identification of the appropriate upper linker for the macrocycle. The P' N-H makes a key hydrogen bonding contact to a conserved water (Figure 2A); therefore linkers were designed to maintain this critical interaction. Molecular modeling also indicated that 14 and 15 membered macrocyclic rings were optimal, which focused our efforts on linkers that would maintain this ring size. As such, a series of linkers of different lengths and constitutions were prepared and evaluated in the TF/FVIIa activity assay (Table 1).[15] Linkers of 4-atoms (**3**, **6**, **7**) and 5-atoms in length (**4**, **5**, **8**) were prepared, as they were expected to be optimal based on molecular modeling overlays with **1**. Within the 4-atom linkers, the position of the oxygen was varied (*e.g.* **3**, **6**) until it was discovered that removal of the oxygen altogether (amide linker, **7**) resulted in a significant improvement in binding affinity. The lower activity of **4** may originate from strain of the bound conformation in which the ester portion of the carbamate is twisted out of plane, as observed in the crystal structure of compound **4** bound to FVIIa (Figure 2).[28-32] Removal of the oxygen, as in the amide system **7**, eliminates this penalty and possibly accounts for the improved potency (See Figure 3 depicting the crystal structure of **7** bound to FVIIa). Furthermore, heteroatom substitution was evaluated in the 5-atom linker series, which revealed that the urea linker (**8**) was significantly more potent. In contrast to the carbamates, the urea does not pay a similar thermodynamic penalty to adopt this strained conformation, which can account for the favorable impact on potency. From these results, the urea (**8**) and amide (**7**) linkers were selected for further optimization due to their promising potency. We elected to optimize the urea linker first due to its superior potency relative to the amide linker.

Table 1. Upper Linker Optimization

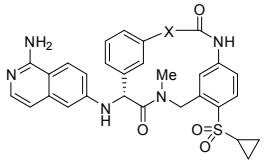

cmpd	X	TF/FVIIa K_i 25 °C (nM)[a]	TF/FVIIa K_i 37 °C (nM)[a,c]
3	$-CH_2O-$	260	
4	$-CH_2CH_2O-$	190	
5	$-CH_2OCH_2-$[b]	23	
6	$-OCH_2-$	710	
7	$-CH_2CH_2-$	<5	58
8	$-CH_2CH_2N(CH_3)-$		6.3

[a]TF/FVIIa K_i values were obtained from recombinant human enzyme and were averaged from two experiments.[15] [b]Contains 4-OMe on the P2 aromatic ring. [c]During the course of optimizations, the assay was modified to 37 °C to better approximate physiological conditions.

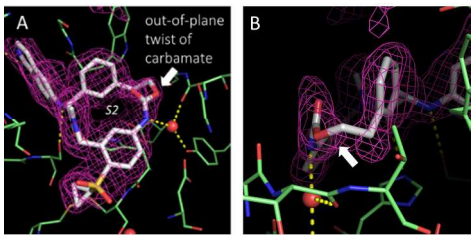

Figure 2. A. Crystallographic structure of compound **4** bound to FVIIa determined at 1.9 Å resolution. The Fo-Fc omit electron density map is depicted at 3 RMSD.[33-34] B. Side view of the strained carbamate substructure. Graphics were generated using the program PyMol.[35]

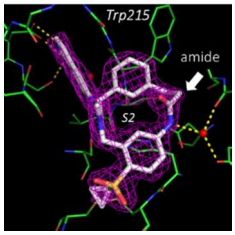

Figure 3. Crystallographic structure of compound **7** bound to FVIIa determined at 1.85 Å resolution. The Fo-Fc omit electron density map is depicted at 3 RMSD.[33-34] Graphics were generated using the program PyMol.[35]

Molecular modeling revealed the presence of a hydrophobic binding pocket near the C-4 position of the P2-phenyl ring, which the unsubstituted analogues were not able to contact (*vide supra*) as shown in Figure 4. It was hypothesized that substitution on the urea nitrogen could potentially improve the binding affinity by contacting the hydrophobic binding pocket above the P2 aryl ring. Additionally, the 4-fluoroaminoisoquinoline P1 moiety was incorporated due to its favorable impact on permeability.[26] Disappointingly, a variety of substitutions at the urea nitrogen actually led to a decrease in potency (**10**-**13**). Unable to improve the potency *via* interactions with the P2 hydrophobic pocket from the urea nitrogen, further inspiration was drawn from the binding model and substitution at the P2 benzylic position. Modeling suggested that *para*-methoxy and benzylic substitution might better fill the S2 pocket, so the *para*-methoxy derivatives with both enantiomers of the corresponding benzylic methyl groups were prepared. Gratifyingly, compound **14** exhibited greatly improved potency when compared to the unsubstituted compound. However the metabolic stability was poor across the series of urea-based macrocycles and rat oral exposure of compound **10** was extremely low (PAMPA pH 7.4 = 220 nm/s, rat po exposure below the limits of quantitation), which led to the decision to discontinue the work on the urea series and turn attention to the amide upper linker for further optimization.

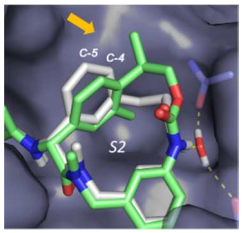

Figure 4. Overlay of crystal structure of the des-fluoro analogues of **1**[25] and model of **16** bound in FVIIa. Graphics were generated using the program PyMol.

Table 2. Urea Optimization

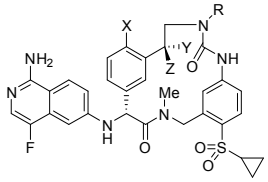

cmpd	X	Y	Z	R	TF/FVIIa K_i 25 °C (nM)	TF/FVIIa K_i 37 °C (nM)	H,RLM $t_{1/2}$ (min)
9	H	H	H	H	17	-	-,-
10	H	H	H	Me	14	200	5,6
11	H	H	H	Bn	80	-	-,-
12[a]	H	H	H	CH_2cPr	59	-	5,12
13[a]	H	H	H	CH_2cBu	150	-	-,-
14	OMe	Me	H	Me	<5	3.8	4,4
15[a,b]	OMe	H	Me	Me	47	-	6,6

[a]Racemic at the phenylglycine center. [b]des-Fluoro analogue of the aminoisoquinoline.

In a manner analogous to the urea upper linkers, it was reasoned that substitution of the P2-aryl ring could improve the potency by interactions with the hydrophobic binding pocket. As such, amide-linked macrocycles containing substituted P2-aryl rings were prepared and evaluated, the results of which are delineated in Table 3. It was discovered that substitution at the C-4 position led to approximately a ten-fold improvement in TF/FVIIa potency (*e.g.* **18**, **21**, **22**, vs **16**). Conversely, substitution at the C-5 position had little to no effect on potency (**19**), presumably because this position is solvent exposed and substituents are not directed into the binding pocket. Monosubstitution at the C-4 position provided relatively flat potency SAR in both the TF/FVIIa and FVIIa deficient prothrombin time assays (anti-clotting assay in human plasma, expressed as the concentration required to prolong clotting time by two-fold), but it modulated rat metabolic stability (as judged by half-life in rat liver microsomes). Providing an appropriate balance between potency and metabolic stability, the difluoroethoxy substitution (**21**) was selected for further optimization.

Table 3. Amide optimization: P2 aryl

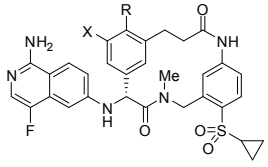

cmpd	X	R	TF/FVIIa K_i 37 °C (nM)	FVII def. PT EC_{2X} (μM)[a]	H,RLM $t_{1/2}$ (min)	PAMPA pH 7.4,5.5 (nM/s)
16	H	H	260	10	13,33	120,67
17	H	F	210	26	-,-	-,-
18	H	OMe	18	11	14,16	540,350
19	OMe	H	290	14	15,46	290,15
20	H	*c*Pr	77	26	26,5	-,-
21	H	OCH_2CHF_2	27	15	32,64	-,88
22	H	OCH_2cPr	26	29	23,23	-,-
23	H	OH	92	14	-,-	-,-
24	F	OMe	410	41	14,8	-,-

[a]See reference 15 for a detailed description of the FVII-deficient prothrombin time assay.

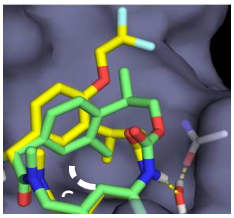

Figure 5. Overlay of crystallographic structures of the des-fluoro analogue of compound **1**[25] (green) and **26** (yellow) bound in FVIIa. Graphics were generated using the program PyMol.

Additional modeling suggested that the amide upper linker may not optimally fill the S2 binding pocket, and we hypothesized that a methyl substituent at the benzylic position in the proper stereochemical orientation should improve this binding interaction, analogous to the urea series (*vide supra*). Both enantiomers of the macrocycle containing the benzylic methyl group were prepared (Table 4), and it was discovered that the (*R*)-enantiomer (**26**, assigned by X-ray co-crystal structure, Figure 5) was significantly more potent than the (*S*)-enantiomer (**25**), resulting in a 100-fold increase in TF/FVIIa potency over the unsubstituted compound (**21**) (see Figure 5), with concomitant improvement in the FVIIa deficient prothrombin time assay. Selected compounds from this series were studied in rat oral PK once promising potency, permeability, and metabolic stability was achieved. Compounds **16** and **18** demonstrated very low (3.7 F%) or no rat oral exposure, respectively, despite reasonable permeability (PAMPA assay). While excellent potency against FVIIa and improved metabolic stability were achieved with compound **26**, off-target liabilities, namely poor tissue kallikrein selectivity and poor rat PK within this series limited its ability to progress further.

Table 4. Amide optimization: benzylic substitution

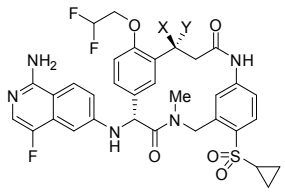

cmpd	X	Y	TF/FVIIa K_i 37 °C (nM)	TK1 K_i (nM)	aPC K_i (nM)	FVII def. PT EC_{2X} (μM)	H,RLM $t_{1/2}$ (min)	PAMPA pH 7.4,5.5 (nM/s)

21	H	H	27	140	1200	15	32,64	-,88
25	Me	H	67	23	5700	23	14,74	-,-
26	H	Me	0.24	9.4	39	3.5	31,39	-,-

Scheme 1. Representative synthesis of compound 18

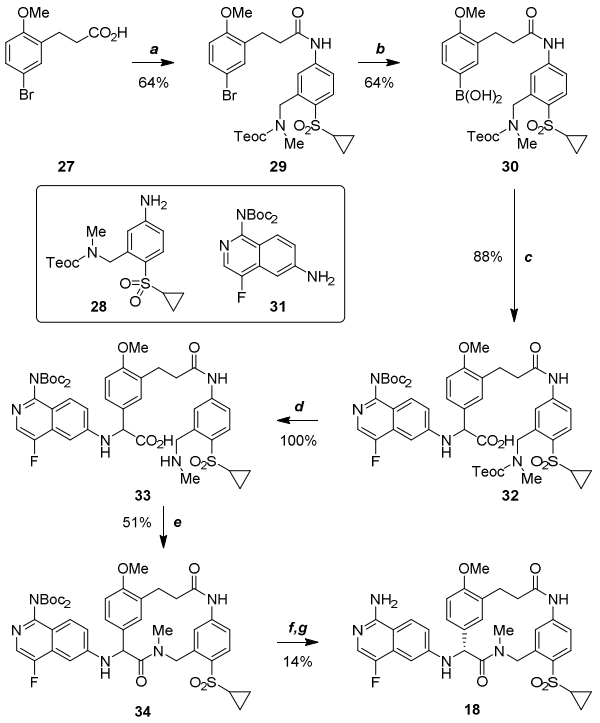

a. $(COCl)_2$ (1.1 equiv.), DMF (0.1 equiv.), DCM, 30 min.; DMAP (0.1 equiv.), TEA (1 equiv.), **28** (1.5 equiv.), 16 h.; *b*. KOAc (2.5 equiv.), bis(neopentyl glycolato)diboron (1.4 equiv.), $PdCl_2$(dppf) (0.1 equiv.), DMSO, 1,4-dioxane, 90 ^oC, 3 h.; *c*. $CHOCO_2H•H_2O$ (1 equiv.), **31** (1 equiv.), DMF, MeCN, 60 ^oC, 16 h.; *d*. TBAF (10 equiv.), THF, 3 h.; *e*. BOP (2 equiv.), DMAP (4 equiv.), DIPEA (10 equiv.), DMF, DCM, 10 hour inverse addition.; *f*. Chiral HPLC; *g*. TFA.

Synthesis of the macrocyclic analogues involved two key steps: 1) Petasis reaction of a functionalized P2 boronic acid to form the phenyl glycine core, and 2) macrocyclization of either the lower amide or upper linker amide, carbamate, or urea. Synthesis of the amide macrocycles was typically accomplished *via* late stage lower amide macrocyclization (Scheme 1). As such, the sequence began with preparation of the appropriately substituted P2 acids according to modifications of literature protocols and known chemistry (**27**). Formation of the upper linker amide bond was achieved via conversion of the acid **27** to the corresponding acid chloride followed by base-mediated coupling with aniline **28** to afford intermediate **29**. The requisite boronic acid **30** was prepared using Suzuki-Miyaura borylation conditions, which set the stage for the key Petasis reaction. Condensation of the protected P1 aniline **31** with glyoxylic acid and boronic acid **30** smoothly provided the desired phenyl glycine core (**32**) in good yield. Deprotection of **32** to provide amine **33** provided the necessary intermediate for the final macrocycle formation. Successful macrocyclization required slow inverse addition of **33** to a solution of the coupling reagents to provide good yields of the desired macrocycle **34**. Final chiral separation and deprotection provided compound **18** in 14% yield over two steps. The lower yield of this two-step sequence is primarily attributed to the material loss upon chiral separation (50%) and final HPLC purification of the unprotected amidine.

Scheme 2. Representative synthesis of compound 10

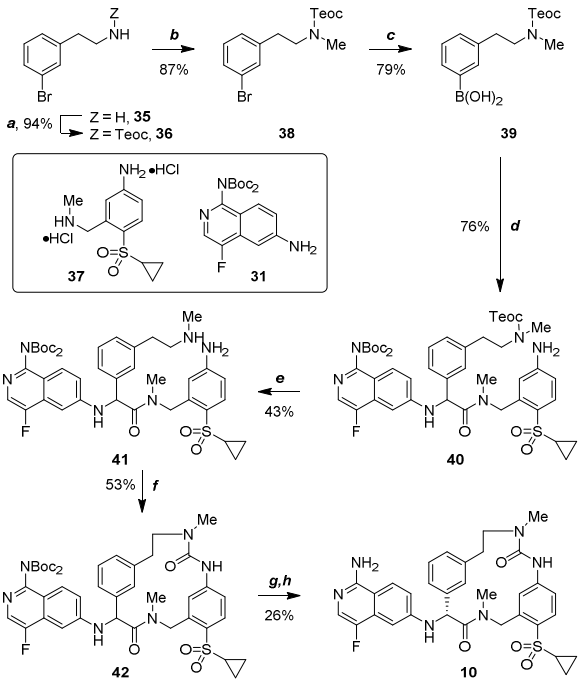

a. p-NO_2-PhOTeoc (1 equiv.), DIPEA (1.2 equiv.), MeOH, 2 h.; *b*. NaH (1.5 equiv.), DMF, 15 min.; MeI, 16 h.; *c*. KOAc (2.5 equiv.), bis(neopentyl glycolato)diboron (1.1 equiv.), PdCl2(dppf) (0.05 equiv.), DMSO, 1,4-dioxane, 90 ^oC, 4 h.; *d*. $CHOCO_2H•H_2O$ (1 equiv.), **31** (1 equiv.), DMF, MeCN, 60 ^oC, 16 h.; **37** (1.3 equiv.), DIPEA (5 equiv.), BOP (1 equiv.), 23 ^oC, 3 h.; *e*. TBAF (10 equiv.), THF, 3 h.; *f*. Pyr (10 equiv.), p-NO_2PhOCOCl (5 equiv.), DCM, 0 to 23 to 50 ^oC, 16 h.; *g*. Chiral HPLC; *h*. TFA.

Efficient access to the urea containing macrocycles was more difficult and required extensive optimization of the synthetic route to access the final compounds in good yield. Scheme 2 delineates this optimized route. Beginning with the amine **35**, installation of a Teoc protecting group and alkylation of the resulting amine generated intermediate **38**. Boronic acid installation (**39**), Petasis reaction and subsequent amine formation proceeded smoothly to generate intermediate **40**. Removal of the Teoc protecting group provided **41** and set the stage for the key macrocyclization reaction. Extensive optimization eventually revealed that formation of the activated carbamate under carefully controlled conditions (5 equivalents of p-NO_2Ph-OCOCl and 10 equivalents of pyridine, 0 to 23 to 50 ^oC) could effect smooth urea formation in good yield to give **42**. Chiral separation and deprotection provided compound **10**.

In conclusion, a series of factor VIIa inhibitors were designed and prepared in order to address the poor rodent metabolic stability and oral exposure of compound **1**. The *meta*-linked macrocyclic series of factor VIIa inhibitors was designed based on careful modeling of the VIIa active site. Using the information garnered through this analysis, the potency of these novel inhibitors was improved from sub-micromolar to sub-nanomolar with concurrent improvement in rodent met-

abolic stability; however, the compounds were not able to solve the larger issues of tissue kallikrein selectivity and poor rodent PK, which precluded further advancement of the series.

ASSOCIATED CONTENT

Supporting Information

Synthesis and characterization data of key compounds. The Supporting Information is available free of charge on the ACS Publications website.

AUTHOR INFORMATION

Corresponding Author

* E-mail: jeremy.richter@bms.com

Notes

The authors declare no competing financial interest.

ACKNOWLEDGMENT

We thank Jeff Bozarth and Mojgan Abousleiman for help in obtaining the enzyme inhibition data referenced herein. We thank Frank Barbera and Yiming Wu for help in obtaining the clotting assay data reference herein. We thank colleagues at the BMS-Biocon Research Center for synthesis of intermediates **31** and **37**. We thank Mei-Mann Hsueh and colleagues at the Biocon-BMS Research Center for performing the PK studies referenced herein. We thank Steven Sheriff both for preparing the coordinates and data of compounds **4**, **7**, and **26** complexed to factor VIIa and depositing them in the PDB.

ABBREVIATIONS

FVIIa, Factor VIIa; TF, Tissue Factor; H,RLM, human, rat liver microsome metabolic stability; PAMPA, parallel artificial membrane permeability assay; TK1, tissue kallikrein-1; aPC, activated protein C; PK, pharmacokinetic; FIX, Factor IX; FIXa, Factor Ixa; FVIIIa, Factor VIIIa; FX, Factor X; Fxa, Factor Xa; DMF, *N*,*N*-dimethylformamide; DCM, dichloromethane; DMAP, dimethylamino pyridine; DMSO, dimethylsulfoxide; TBAF, tetra-*N*-butylammonium fluoride; THF, tetrahydrofuran; BOP, (Benzotriazol-1-yloxy)tris(dimethylamino)phosphonium hexafluorophosphate; DIPEA, diisopropylethylamine; HPLC, high performance liquid chromatography; TFA, trifluoroacetic acid; HATU, 1-[Bis(dimethylamino)methylene]-1H-1,2,3-triazolo[4,5-b]pyridinium 3-oxidhexafluorophosphate; NMM, N-methylmorpholine.

REFERENCES

(1) Global Status Report on Noncommunicable Diseases 2010; WHO Press: Geneva, 2011.

(2) Furie, B.; Furie, B. C. Mechanisms of Thrombus Formation. *New Engl. J. Med.* **2008**, *359*, 938 – 949.

(3) Mackman, N.; Tilley, R. E.; Key, N. S. Role of the Extrinsic Pathway of Blood Coagulation in Hemostasis and Thrombosis. *Arterioscler. Thromb. Vasc. Biol*. **2007**, *27*, 1687 – 1693.

(4) De Caterina, R. *et. al. J. Am. Coll. Cardiol.* New Oral Anticoagulants in Atrial Fibrillation and Acute Coronary Syndromes **2012**, *59*, 1413 – 1425.

(5) Lee, A.; Agnell, G.; Buller, H.; Ginsbert, J.; Heit, J.; Rote, W.; Vlasuk, G.; Costantini, L.; Julian, J.; Comp, P.; va der Meer, J.; Piovella, F.; Raskob, G.; Gent, M. Dose-Response Study of Recombinant Factor FVIIa/Tissue Factor Inhibitor Recombinant Nematode Anticoagulant Protein c2 in Prevention of Postoperative Venous Thromboembolism in Patients Undergoing Total Knee Replacement. *Circulation*, **2001**, *104*, 75 – 78.

(6) Moons, A. H. M,; Peters, R. J. G.; Bijsterveld, N. R.; Piek, J. J.; Prins, M. H.; Vlasuk, G. P.; Rote, W. E.; Buller, H. R. Recombinant Nematode Anticoagulant Protein c2, an Inhibitor of the Tissue Factor/Factor FVIIa Complex, in Patients Undergoing Elective Coronary Angioplasty. *J. Am. Coll. Cardiol*. **2003**, *41*, 2147 – 2153.

(7) Giugliano, R. P.; Wiviott, S. D.; Stone, P. H.; Simon, D. Si.; Schweiger, M. J.; Bouchard, A.; Leesar, M. S.; Goulder, M. A.; Deitcher, S. R.; McCabe, C. H.; Braunwald, E. Recombinant Nematode Anticoagulant Protein c2 in Patients with non-ST-Segment Elevation Acute Coronary Syndrome: the ANTHEM-TIMI-32 Trial. *J. Am. Coll. Cardiol.* **2007**, *49*, 2398 – 2407.

(8) Suleymanov, O. D.; Szalony, J. A.; Salyers, A. K.; Lachance, R. M.; Parlow, J. J.; South, M. S.; Wood, R. S.; Nicholson, N. S. Pharmacological Interruption of Acute Thrombus Formation with Minimal Hemorrhagic Complications by a Small Molecule Tissue Factor/Factor FVIIa Inhibitor: Comparison to Factor Xa and Thrombin Inhibition in a Nonhuman Primate Thrombosis Model. *J. Pharmacol. Exp. Ther.* **2003**, *306*, 1115 – 1121.

(9) Szalony, J. A.; Suleymanov, O. D.; Salyers, A. K.; Panser-Knodle, S. G.; Blom, J. D.; LaChance, R. M.; Case, B. L.; Parlow, J. J.; South, M. S.; Wood, R. S.; Nicholson, N. S. Administration of a Small Molecule Tissue Factor/Factor VIIa Inhibitor in a non-Human Primate Thrombosis Model of Venous Thrombosis: Effects on Thrombus Formation and Bleeding Time. *Thromb. Res.* **2003**, *112*, 167 – 174.

(10) Salyers, A. K.; Szalony, J. A.; Suleymanov, O. D.; Parlow, J. J.; Wood, R. S.; South, M. S.; Nicholson, N. S. Assessment of Bleeding Propensity in non-Human Primates by Combination of Selective Tissue Factor/VIIa Inhibition and Aspirin Compared to Warfarin and Aspirin Treatment. *Pharmacology*, **2004**, *70*, 100 – 106.

(11) Olivero, A. G.; Eigenbrot, C.; Goldsmith, R.; Robarge, K.; Artis, D. R.; Flygare, J.; Rawson, T.; Sutherlin, D. P.; Kadkhodayan, S.; Beresini, M.; Elliot, L. O.; DeGuzman, G. G.; Banner, D. W.; Ultsch, M.; Marzec, U.; Hanson, S. R.; Refino, C.; Bunting, S.; Kirchhofer, D. W. A Selective, Slow Binding Inhibitor of Factor FVIIa Binds to a Nonstandard Active Site Conformation and Attenuates Thrombus Formation in vivo. *J. Biol. Chem.* **2005**, *280*, 9160 – 9169.

(12) Young, W. B.; Mordenti, J.; Torkelson, S.; Shrader, W. D.; Kolesnikov, A.; Rai, R.; Liu, L.; Hu, H.; Leahy, E. M.; Green, M. J.; Sprengler, P. A.; Katz, B. A.; Yu, C.; Janc, J. W.; Elrod, K. C.; Marzec, U. M.; Hanson, S. R. Factor VIIa Inhibitors: Chemical Optimization, Preclinical Pharmacokinetics, Pharmacodynamics, and Efficacy in an Arterial Baboon Thrombosis Model. *Bioorg. Med. Chem.* **2006**, *16*, 2037 – 2041.

(13) Zbinden, K. G.; Banner, D. W.; Hilpert, K.; Himber, J.; Lavé, T.; Riederer, M. A.; Stahl, M.; Tschopp, T. B.; Obst-Sander, U. Dose-Dependent Antithrombotic Activity of an Orally Active Tissue Factor/Factor VIIa Inhibitor without Concomitant Enhancement of Bleeding Propensity. *Bioorg. Med. Chem.* **2006**, *14*, 5357 – 5360.

(14) Arnold, C. S.; Parker, C.; Upshaw, R.; Prydz, H.; Chand, P.; Kotian, P.; Bantia, S.; Babu, Y. S. The Antithrombotic and Anti-Inflammatory Effects of BCX-3607, a Small Molecule Tissue Factor/Factor VIIa Inhibitor. *Thromb. Res.* **2006**, *117*, 343 – 349.

(15) Wong, P. C.; Luettgen, J. M.; Rendina, A. R.; Kettner, C. A.; Xin, B.; Knabb, R. M.; Wexler, R. R.; Priestley, E. S. BMS-593214, an Active Site-Directed Factor FVIIa Inhibitor: Enzyme Kinetics, Antithrombotic and Antihaemostatic Studies. *Thromb. Haemostasis*, **2010**, *104*, 261 – 269.

(16) Robinson, L.A. ; Saiah, E. M. K. Anticoagulants : Inhibitors of the Factor VIIa/Tissue Factor Pathway. *Annu. Rep. Med. Chem.* **2002**, *37*, 85 – 98.

(17) Lazarus, R. A. ; Olivero, A. G. ; Eigenbrot, C. ; Kirchhofer, D. Inhibitors of Tissue Factor.Factor VIIa for Anticoagulant Therapy. *Curr. Med. Chem.* **2004**, *11*, 2275 – 2290.

(18) Frederick, R. ; Pochet, L. ; Charlier, C. ; Masereel B. Modulators of the Coagulation Cascade : Focus and Recent Advances in Inhibitors of Tissue Factor, Factor VIIa and Their Complex. *Curr. Med. Chem.* **2005**, *12*, 397 – 417.

(19) Shirk, R. A., Vlasuk, G. P. Inhibitors of Factor FVIIa/Tissue Factor. *Arterioscler. Thromb. Vasc. Biol.* **2007**, *27*, 1895 – 1900.

(20) Priestley, E. S. Tissue Factor-FVIIa Inhibition : Update on an Unfinished Quest for a Novel Oral Antithrombotic. *Drug Discov. Today.* **2014**, *19*, 1440 – 1444.

(21) Riggs, J. R.; Kolesnikov, A.; Hendrix, J.; Young, W. B.; Shrader, W. D.; Vijaykumar, D.; Stephens, R.; Liu, L; Pan, L.; Mordenti, J.; Green, M. J.; Sukbuntherng, J. Factor VIIa Inhibitors: A Prodrug Strategy to Improve Oral Bioavailability. *Bioorg. Med. Chem. Lett.* **2006**, *16*, 2224 – 2228.

(22) Vijaykumar, D.; Rai, R.; Shaghafi, M.; Ton, T.; Torkelson, S.; Leahy, E. M.; Riggs, J. R.; Hu, H.; Sprengeler, P. A.; Shrader, W. D.; O'Bryan, C.; Cabuslay, R.; Sanford, E.; Gjerstadt, E.; Liu, L.; Sukbuntherng, J.; Young, W. B. Efforts Towards Oral Bioavailability in Factor VIIa Inhibitors. *Bioorg. Med. Chem. Lett.* **2006**, *16*, 3829 – 3832.

(23) Zbinden, K. G.; Obst-Sander, U.; Hilpert, K.; Kuehne, H.; Banner, D. W.; Boehm, H.-J.; Stahl, M.; Ackermann, J.; Alig, L.; Weber, L. Selective and Orally Bioavailable Phenylglycine Tissue Factor/Factor VIIa Inhibitors. *Bioorg. Med. Chem. Lett.* **2005**, *15*, 5344 – 5352.

(24) Priestley, E. S.; Cheney, D. L.; DeLucca, I.; Wei, A.; Luettgen, J. M.; Rendina, A. R.; Wong, P. C.; Wexler, R. R. Structure-Based Design of Macrocyclic Coagulation Factor VIIa Inhibitors. *J. Med. Chem.* **2015**, *58*, 6225 – 6236.

(25) Glunz, P. W.; Mueller, L.; Cheney, D. L.; Ladziata, V.; Zou, Y.; Wurtz, N. R.; Wei, A.; Wong, P. C.; Wexler, R. R.; Priestley, E. S. Atropisomer Control in Macrocyclic Factor VIIa Inhibitors. *J. Med. Chem.* **2016**, *59*, 4007 – 4018.

(26) Zhang, X.; Glunz, P. W.; Johnson, J. A.; Jiang, W.; Jacutin-Porte, S.; Ladziata, V.; Zou, Y.; Phillips, M. S.; Wurtz, N. R.; Parkhurst, B.; Rendina, A. R.; Harper, T. M.; Cheney, D. L.; Luettgen, J. M.; Wong, P. C.; Seiffert, D.; Wexler, R. R.; Priestley, E. S. Discovery of a Highly Potent, Selective, and Orally Bioavailable Macrocyclic Inhibitor of Blood Coagulation Factor VIIa-Tissue Factor Complex. *J. Med. Chem.* **2016**, *59*, 7125 – 7137.

(27) For a review of the use of macrocycles in drug discovery, please see: Marsault, E.; Peterson, M. L. Macrocycles Are Great Cycles: Applications, Opportunities, and Challenges of Synthetic Macrocycles in Drug Discovery. *J. Med. Chem.* **2011**, *54*, 1961 – 2004, and references therein.

(28) A search of the Cambridge Crystallographic Database showed that the ester portion of carbamates having a similar substitution pattern as **2** overwhelmingly adopt an *s-trans*-configuration.

(29) Bruno, I. J.; Cole, J. C.; Edgington, P. R.; Kessler, M.; Macrae, C. F.; McCabe, P.; Pearson, J.; Taylor, R. New Software for Searching the Cambridge Structural Database and Visualizing Crystal Structures. *Acta Crystallogr. B.* **2002**, *58 (Pt 3 Pt 1)*, 389 – 397.

(30) Brameld, K. A.; Kuhn, B.; Reuter, D. C.; Stahl, M. Small Molecule Conformational Preferences Derived from Crystal Structure Data. A Medicinal Chemistry Focused Analysis. *J. Chem. Inf. Mod.* **2008**, *48*, 1 – 24.

(31) Böhm, J.-J.; Klebe, G. What Can We Learn from Molecular Recognition in Protein-Ligand Complexes for the Design of New Drugs? *Angew. Chem. Int. Ed. Eng.* **1996**, *35*, 2588 – 2416.

(32) Pawar, D. M.; Khalil, A. A.; Hooks, D. R.; Collins, K.; Elliott, T.; Stafford, J.; Smith, L.; Noe, E. A. *E* and *Z* Conformations of Esters, Thiol Esters, and Amides. *J. Am. Chem. Soc.* **1998**, *120*, 2108 – 2112.

(33) Structures were determined by soaking crystals of des-Gla factor VIIa in complex with benzamidine with each of the inhibitors. For further details, see Supporting Information.

(34) Relative atomic coordinates for the crystallographic structures of **4**, **7**, and **26** complexed with factor VIIa have been deposited in the PDB; their deposition numbers are 5TQE, 5TQF, 5TQG, respectively.

(35) The PyMOL Molecular Graphics System, Version 1.7.2, Schrödinger, LLC.